Orientation of individual C_{60} molecules adsorbed on Cu(111): Low-temperature scanning tunneling microscopy and density functional calculations

J. Andreas Larsson,[1,*] Simon D. Elliott,[1] James C. Greer,[1] Jascha Repp,[2,3] Gerhard Meyer,[2] and Rolf Allenspach[2]
[1]*Tyndall National Institute, Lee Maltings, Prospect Row, Cork, Ireland*
[2]*IBM Research, Zurich Research Laboratory, CH-8803 Rüschlikon, Switzerland*
[3]*Institute of Experimental and Applied Physics, University of Regensburg, 93040 Regensburg, Germany*
(Received 7 June 2007; revised manuscript received 14 January 2008; published 20 March 2008)

Density functional theory (DFT) and low-temperature scanning tunneling microscopy (STM) have been combined to examine the bonding of individual C_{60} molecules on Cu(111). Energy-resolved differential-conductance maps have been measured for individual C_{60} molecules adsorbed on a Cu(111) surface by means of low-temperature STM, which are compared to and complemented by theoretically computed spectral images. It has been found that C_{60} chemisorbs with a six-membered ring parallel to the surface at two different Cu(111) binding sites that constitute two exclusive hexagonal sublattices. On each sublattice, C_{60} is bonded in one particular rotational conformer, i.e., C_{60} molecules bind to the Cu(111) surface in two different azimuthal orientations differing by 60° depending on which sublattice the binding site belongs to. The binding conformation of C_{60} and its orientation with regard to the copper surface can be deduced by this joint experimental-theoretical approach. Six possible pairs of C_{60} configurations on three different Cu surface binding sites have been identified that fulfil the requirements of the two sublattices and are consistent with all experimental and theoretical data. Theory proposes that two of these configuration pairs are most likely. We have found that DFT does not get the binding energy between rotational conformers in the correct order. We also report two different C_{60} monolayers on Cu(111): one with alternating orientations of neighboring molecules at low temperature and the other with (4×4) structure after annealing above room temperature.

DOI: 10.1103/PhysRevB.77.115434 PACS number(s): 73.20.−r, 73.22.−f, 71.20.Tx

I. INTRODUCTION

The continued interest in C_{60} molecules adsorbed on metal surfaces stems from their unique structure and chemical properties and from their potential use in molecular electronics.[1–5] For the latter, a knowledge of the bonding and electronic structure of individual molecules adsorbed on metals is essential. For a detailed understanding of the bonding and electronic structure, in turn, a knowledge of the binding site is fundamental.

Whereas numerous previous experimental and theoretical studies of the adsorption of monolayers of C_{60} on metal surfaces have been carried out, very little is known about the adsorption geometry of individual molecules[2,4,6,7] on these surfaces. In this work, we focus on the bonding of individual C_{60} molecules on Cu(111) and discuss the challenges that arise in this context.

In general, the bonding of C_{60} can be categorized by three different independent parameters: (i) what part of the cage bonds to the surface (polar angle), (ii) what part of the surface the cage bonds to (binding site), and (iii) the rotational orientation of the cage (azimuthal angle). The determination of these bonding parameters is each connected with its own difficulties. In scanning tunneling microscopy (STM), for instance, the polar angle may be readily determined from the symmetry of the images. However, there are several problems concerning the determination of the binding site: The Cu(111) surface is very flat and therefore does not allow a direct determination of binding sites from atomically resolved STM images, it has several different binding sites that barely differ in height, and the different binding sites are only about 1.3 Å apart; the C_{60} molecule is sufficiently large that even a small coupling of lateral and vertical movement in the instrument can easily falsify a direct site determination.

At first glance, one could simply expect that the binding geometry of individual C_{60} molecules on Cu(111) might be similar or even the same as that for a monolayer film. Therefore, we briefly review the observations to date for monolayers of C_{60} on Cu(111).

In early publications, it was observed that the annealing of monolayers well above room temperature leads to a very well ordered (4×4) structure, in which all the C_{60} molecules are oriented in the same way.[8–11] Therefore, a similar surface preparation has been applied in most subsequent studies to obtain well-ordered monolayer films and a variety of experimental methods have then been applied to study these films.[8,9,11–20] From the corresponding STM images,[8,9,11,20–22] it was concluded from the threefold molecular symmetry that the fullerenes were oriented with a six-membered ring toward the surface. Binding was argued to be on hollow sites of the surface from an observed lateral shift between neighboring domains. More specifically, these studies suggested that within one domain, the site was always the same, but with both the fcc-hollow and hcp-hollow sites occurring in different domains. This was later contradicted by Pai *et al.*[23] by using similar methods (as discussed below). Using x-ray photoelectron diffraction (XPD), Fasel *et al.*[12] also found that C_{60} on Cu(111) bonds with a six-membered ring oriented to the metal surface, with the molecules in two different equivalent azimuthal orientations. Fartash[13] described two types of monolayer C_{60} on Cu(111) with respect to the binding site for C_{60}. They reported that the cages are either all bonded above an on-top site, or one-third each bound

above an on-top site, an hcp-hollow site, and an fcc-hollow site.

Theoretical results were obtained by Wang and Cheng[24] from density functional theory (DFT) calculations for periodic cell models in the local density approximation (LDA). As previous experiments reported a (4×4) adsorption structure, in which all the C_{60} molecules were oriented the same way, Wang and Cheng studied the adsorption site under the constraint of a (4×4) structure with the fullerene six-membered ring oriented toward the surface. They found bonding to the hcp-hollow site lowest in energy, bonding to the bridge, and fcc-hollow sites only 20 meV higher in energy and bonding to the on-top site higher by 240 meV. They also studied the rotational orientation of C_{60} on each of these binding sites. The theoretical study of Ogawa *et al.*[25] using DFT with a generalized gradient approximation (GGA) hybrid functional considered bonding of several polar angles and azimuthal orientations of the C_{60} molecule relative to the on-top site of Cu(111) and found the most stable to be a polar angle orientation with a C-C partial double bond between two six-membered rings (a six-six bond) directed toward the surface. However, the binding energies for all configurations considered in their study, including a configuration with a six-membered ring oriented toward the surface, were within 500 meV of one another.

More recently, it was discovered that deposition and/or annealing temperatures well above room temperature resulted in substantial reconstructions of the underlying substrate surface and thus in rough interface geometries. Such reconstruction patterns were first observed for C_{60} monolayers on more open metal surfaces,[10,26–28] but later also for (111)-oriented metal surfaces,[29,30] including Cu(111).[23] Most recently, Stróżecka *et al.*[31] have studied small islands of C_{60} molecules on Cu(111) by means of STM grown well below room temperature, at which substrate reconstruction could be ruled out. They found two polar angles and concluded that C_{60} either bonds with a six-membered ring or a six-six bond toward the surface.[31]

When consulting the existing literature, as discussed above, it becomes apparent that the geometry of C_{60} in monolayers may not be directly related to the binding of an individual molecule because the former is due to the balance between molecule-molecule and substrate-molecule interactions. Nevertheless, we do compare these results to ours throughout the paper since work on the adsorption of individual C_{60} molecules is very rare. It is also evident that other characteristics of the binding that have been measured after annealing the films to well above room temperature may be related to the rough, reconstructed interface, and are not characteristic for C_{60} molecules on a flat Cu(111) surface. The complications due to surface reconstructions caused by annealing further hamper direct comparison between experimental and theoretical results.

On the other hand, it has been well established in numerous combined STM and DFT studies on individual and monolayer C_{60} how the intramolecular resolution relates to the azimuthal orientation of the molecules on a variety of different surfaces,[6,8,11,32–38] and so this aspect of the molecular bonding can be readily obtained.

In this paper, we perform STM scans, STM-manipulation-assisted site determination[39] of C_{60} molecules on Cu(111), and molecular STM $I(V)$ measurements including scanning tunneling spectroscopy (STS) differential conductance (dI/dV) spectral images. We also perform DFT calculations in order to interpret these experiments. The spatial mapping of the energy-resolved electronic density of single C_{60} molecules on the Ag(100) surface by means of STM and STS has been reported by Lu *et al.*[6] In their work, differential conductance (dI/dV) spectra are mapped over the molecular surface at constant current, allowing the nature of individual C_{60} orbitals bonded to an Ag(100) surface to be examined. A similar mapping of single electron orbitals onto a constant-current surface for C_{60} bonded to Cu(111) is performed in the current work. Several states above (unoccupied) and below (occupied) the Fermi level (E_F) are imaged and compared to DFT calculations. Since the spatial mapping of the energy-resolved electronic density is very sensitive to the nature of C_{60} bonding to Cu(111) as well as the charge transfer between C_{60} and the substrate, this comparison tests whether bonding characteristics deduced from our calculations are applicable to the adsorption state seen in experiment.

We aim to deduce the nature of C_{60} bonding to Cu(111) (chemisorption vs physisorption), the C_{60} polar angle, and the Cu(111) binding site of C_{60} and we seek to establish the azimuthal orientation of C_{60} with regard to the copper surface. We will show that, in particular, the site determination is not easily achievable, but that we can narrow down the possible binding configurations considerably with a combined first-principles computation and low-temperature STM approach. The high symmetry of C_{60} combined with the atomic flatness of the Cu(111) is the reason the fullerene binding is so difficult to experimentally deduce. Theoretically, there are difficulties since the binding involves charge transfer and electron sharing, for which electron correlation is important, but electron correlation is only approximately included in DFT within LDA and GGA formulations. Other more accurate methods are precluded because of the system size. Although there has been a considerable amount of experimental and theoretical efforts to determine C_{60} bonding to Cu(111), a clear picture still has not emerged, and there is a considerable discrepancy between different reports in the literature. We will show that the complexity of the system is such that our combined STM and DFT investigation still leaves room for different possibilities.

II. METHODS

Our experiments were performed with a home-built low-temperature STM operated at 5 K. The Cu(111) single crystal samples are cleaned by sputtering and annealing cycles. C_{60} molecules are deposited by thermal evaporation onto the Cu(111) surface at substrate temperatures of 5 and $\approx$100 K. These temperatures allowed us to study not only the internal structure of individual C_{60} molecules $(T=5$ K) but also the formation of C_{60} islands $(T\approx100$ K) or the adsorption of C_{60} at step edges. Bias voltages refer to the sample voltage with respect to the tip. Lateral manipulation was performed at the largest possible tip-sample distance, at which the molecules still followed the motion of the tip. This means that step by step the tip-sample distance was decreased at a bias voltage

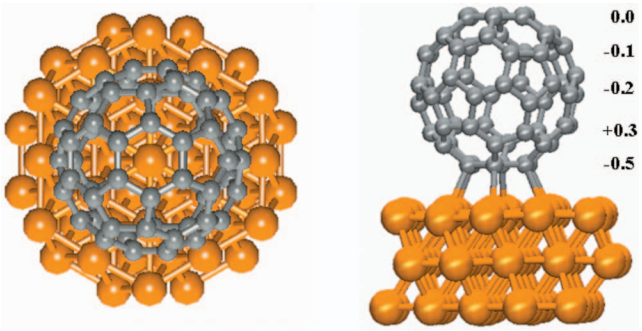

FIG. 1. (Color) Model structure for C_{60} bonded to a Cu(111) surface in top and side views. The copper clusters are composed of 55 atoms. The sum of the Mulliken charges per layer of C_{60} when bonded to copper are given next to the side view representation.

of 50 mV until the molecules started to move. Subsequently, these parameters were used for manipulation.

To relate the experimental STM results to the electronic structure of adsorbed C_{60}, DFT calculations using the Becke–Perdew exchange-correlation functional of GGA[40,41] and a polarized valence double zeta basis[42] have been performed. For the copper atoms, a ten electron relativistic effective core potential is used,[43] leaving 19 electrons per copper atom within the computations. All calculations have been performed using the TURBOMOLE program system.[44,45] We have calculated C_{60} bonded to Cu_{55} "coin-shaped" clusters that are three metal layers thick and wider in the surface direction than the C_{60} molecular diameter, as depicted in Fig. 1.

III. RESULTS AND DISCUSSION

A. Mode of adsorption of C_{60} at Cu(111) from scanning tunneling microscopy, scanning tunneling spectroscopy, and density functional theory

Individual C_{60} molecules deposited at 5 K were imaged by STM. As observed in previous studies, constant-current images of the molecules show a clear intramolecular structure with threefold rotational symmetry (see Fig. 2), thereby indicating that the molecules are bound with a C_3 symmetry axis normal to the copper surface. Thus, the fullerene bonds with a six-membered ring oriented to the copper surface and has another six-membered ring at the "top" of its cage, as was also found for C_{60} monolayers.[8,9,11,12,20,23] We are confident that this verifies the fullerene polar angle but it also has implications for which binding sites on Cu(111) are possible, namely, only trigonally symmetric binding sites. In order to scrutinize the fullerene bonding with regard to binding site and azimuthal orientation, we have thus calculated C_{60} bonded to the three Cu(111) binding sites with trigonal symmetry (on-top, hcp-hollow, and fcc-hollow sites) using DFT, which results in nine different rotational configurations of C_3 and C_{3v} symmetries, as shown in Fig. 3. As can be seen from Table I, we found stable binding for all configurations except for fcc-hollow(I) and fcc-hollow(III) (nomenclature defined in Fig. 3). Weng and Chang[24] on the other hand, calculated rotational potentials for C_{60} on these three sites and have found bound configurations for all rotational angles in a supercell geometry representing a (4×4) monolayer of C_{60}.[24] Their binding energies are also given in Table I for easy reference.

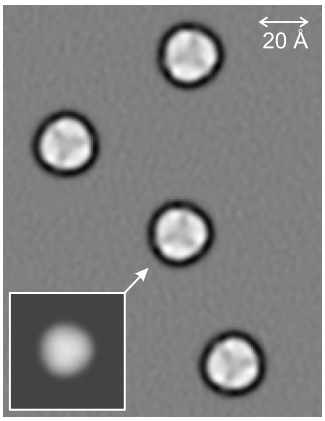

FIG. 2. Individual C_{60} molecules on Cu(111). The image is obtained with a high-pass (Laplace) filter enhancing the intramolecular resolution. The C_{60} molecules show a threefold rotational symmetry and two different orientations with respect to the copper substrate. The inset shows the topography image for a single molecule displayed without high-pass filtering (tunneling parameters $I=3.8\times10^{-11}$ A and $V=1.7$ V).

To establish a direct link between our calculations and experiments, spatial maps of the energy-resolved electronic density have been obtained from STS differential conductance (dI/dV) spectral images and compared to simulated ones. A series of such energy resolved dI/dV maps for individually bound C_{60} molecules in the range of -3.0 to $+2.7$ V were acquired. Out of this series, images corresponding to peaks in local dI/dV spectroscopy, as well as those which show a pronounced intramolecular structure, are

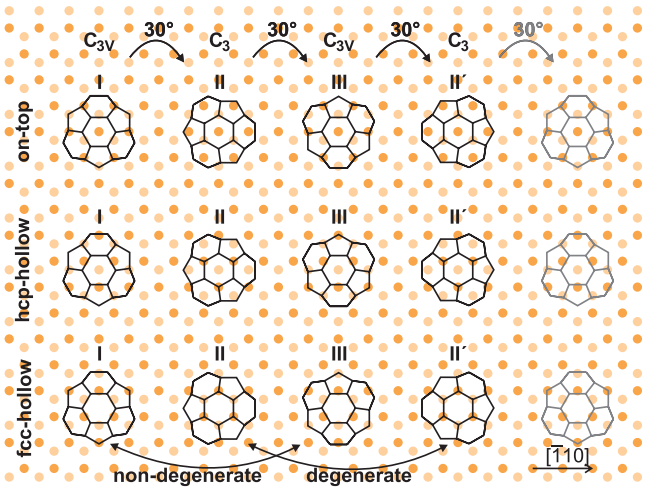

FIG. 3. (Color) All binding configurations of C_{60} on the on-top, hcp-hollow, and fcc-hollow sites of the Cu(111) surface. The structure of the bottom of C_{60} (black lines) with regard to Cu(111) (orange balls, Cu atoms; dark balls, top surface Cu atoms; and light balls, second layer Cu atoms) is shown. The structure of the top of C_{60} relates to the bottom structure by 60° rotation.

TABLE I. Binding energies in eV and bond lengths in Å computed with DFT. C—C(6-5) and C=C(6-6) refer to the partial single and double bonds, respectively, of the C_{60} hexagon bonded to the copper surface.

Property	On-top(I)	On-top(II)	On-top(III)	hcp-hollow(I)	hcp-hollow(II)	hcp-hollow(III)	fcc-hollow(I)	fcc-hollow(II)	fcc-hollow(III)
Sym	C_{3v}	C_3	C_{3v}	C_{3v}	C_3	C_{3v}	C_{3v}	C_3/C_1	C_{3v}
E (bond)	1.617	0.858	1.900	1.091	1.838	0.781		1.240[a]	
E (bond)[b]	(1.98)	(1.71)	2.00	(2.14)	2.24	(1.97)	(1.91)	2.20	(2.12)
C—C(6-5)	1.491	1.499	1.499	1.477	1.482	1.468		1.487, 1.489, 1.495[a]	
C=C(6-6)	1.474	1.448	1.457	1.433	1.450	1.437		1.434, 1.454, 1.459[a]	
Cu—C	2.318	2.280	2.368	2.393	2.214	2.341		2.204, 2.258, 2.263[a]	

[a]In our cluster calculations, fcc(II) is found in a Jahn–Teller distorted C_1 symmetry.
[b]Calculated values from Ref. 24; values in parentheses are reported as rotational maxima, estimated from Fig. 2 in Ref. 24.

shown in Fig. 4. Simulation of these images was performed in a manner similar to the procedure described in Ref. 6, and therefore, will be only briefly described. During the recording of these images, the tip does not scan at a constant distance from the sample but follows a corrugated electron density isosurface, which shifts depending on the bias voltage. Electrons within the energy range between the two Fermi levels of the tip and sample, hereafter referred to as the bias window, contribute to the tunneling current. Consequently, the topography of the electron density at a given bias voltage is not only given by the local density of states (LDOS) arising from a single energy level but also a sum over all orbitals

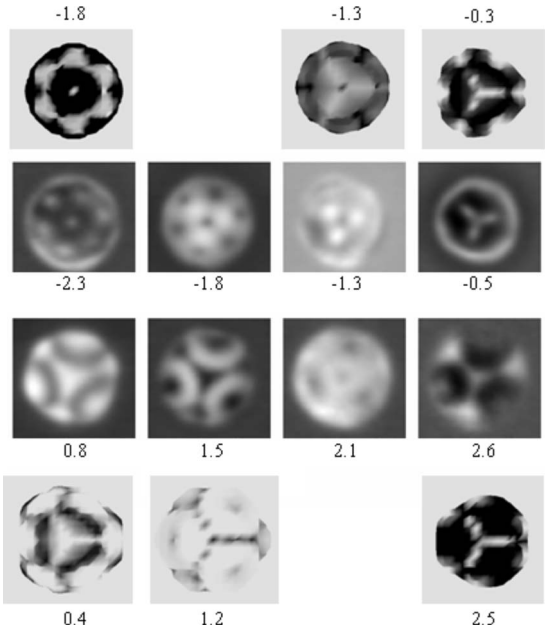

FIG. 4. dI/dV images of C_{60} acquired at constant current mode for a set of voltages (V) are shown in the middle two rows, and the simulated counterparts with Kohn–Sham orbital energies (eV) are in the top and bottom row. Fermi level is at 0 V (eV). The calculated images were obtained for the on-top site, but very similar images have been computed for the hcp-hollow site.

lying within the bias window. The tip then moves in a manner to maintain constant current. In order to compare the electronic structure to a constant-current dI/dV map, it is necessary to first simulate the STM topography image, which is obtained by summing the Kohn–Sham electron densities lying within the bias window. Then, the highest (lowest) orbital's charge density on this constant current surface is plotted on the constant current surface for unoccupied (occupied) states. The resulting orbital image is projected onto a plane for direct comparison with the experimental STM images. This has been done for C_{60} bonded to both the on-top and the hcp-hollow sites, and the resulting images and orbital energy differences are very similar; thus only the on-top data are shown in Fig. 4.

Experimental and theoretical images are displayed next to each other in Fig. 4 for ease of comparison for the experimental bias values and Kohn–Sham eigenvalues of −2.3 V/−1.8 eV, −1.3 V/−1.3 eV, −0.5 V/−0.3 eV, 0.8 V/0.4 eV, 1.5 V/1.2 eV, and 2.6 V/2.5 eV, which should be considered along with the complex highest occupied molecular orbital (HOMO) at E_F (not seen in STS) due to Fermi-level pinning. Positive voltage bias corresponds to tunneling into unoccupied states with fullerene character, whereas negative biases correspond to tunneling from occupied states. We suggest that the measured states at −1.8 and 2.1 V are superpositions of many states with little separation at these energies or interference signals from other states within the bias window. Good overall agreement between measured and computed images is seen. Most of the complex orbital structure observed in experiment is reproduced well by the calculations, in particular, if one considers that the finite size of the STM tip will impose a finite spatial resolution.[46] Moreover, the molecular orientation is clearly reflected by the orbital images. Note that Kohn–Sham eigenvalues underestimate the energy spacing for occupied to unoccupied molecular orbitals, and that there are limitations in directly interpreting the Kohn–Sham eigenfunctions as physical states. The images in Fig. 4 thus map out a C_{60} LDOS of selected states with very good agreement between experiment and theory.

Our combined STS and DFT study shows that C_{60} chemisorbs to the copper surface when deposited at 5 K, as seen

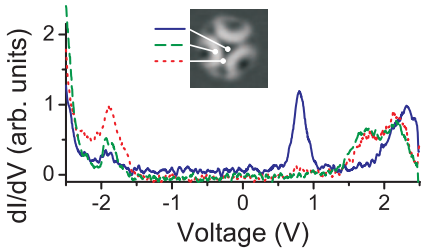

FIG. 5. (Color) Local dI/dV spectroscopy at the center (blue) and at two off-center (dotted red and green lines) positions of a C_{60} molecule. The two off-center positions were 5 Å away from the center in the direction of the pentagons and hexagons of the upper part of the cage, respectively. For easy reference, these positions are marked in the dI/dV image of the inset. The vertical tip position corresponds to feedback parameters of $I=65$ pA at $V=+2155$ mV.

from the pronounced splitting of the C_{60} HOMO and lowest unoccupied molecular orbital (LUMO) derived states in the theoretical energy-resolved differential conductance images of Fig. 4, which have also been identified with one-to-one correspondence in the experimental images. This should be compared to a physisorbed C_{60} that would only have minute HOMO and LUMO level splittings (i.e., no hybridization and no charge transfer). Thus, the comparison between experiment and theory of the spatial mapping of the energy-resolved electronic density is a very sensitive measure to whether or not the adsorption state and charge transfer found in the calculations corresponds to the experimentally observed one. Our good agreement in this case suggests that the nature of bonding and its characteristics as found in theory correspond to the experiment and is the reason we have been able to establish that C_{60} is chemisorbed to Cu(111) with considerable charge transfer.

Two points can be made regarding the C_{60} LUMO derived states. The HOMO of the C_{60}-Cu(111) complex shows characteristics of the pristine C_{60} LUMO, which is thus a measure of the charge transfer to the molecule due to surface bonding. In addition, the structure of the empty state at 1.5 V/1.2 eV allows for a clear identification of what molecular features are seen in the STM images of Fig. 2 since the bright features in the experimental and theoretical images correspond to the five-membered rings around the top of the fullerene, and the orientation in STS spectral images and STM scan images can be correlated, as has been previously observed.[6,8,11,32,33] Thus, both the strength of the fullerene-metal surface bonding and the orientation of the fullerene can be determined directly from the lowest lying C_{60} derived energy levels (corresponding to the fullerene LUMO and LUMO+1) for this and other metal surfaces.

Figure 5 shows local dI/dV spectra acquired directly atop the center of an individual C_{60} molecule as well as for two different off-center positions. The center dI/dV spectrum shows a clear peak at about 0.8 V above E_F and this resonance can be identified as the e state derived from the fullerene LUMO. The fullerene LUMO+1 derived state at 1.5 V has no density at the center (see Fig. 4) and is thus only seen in the off-center dI/dV spectra. In agreement with previous measurements reported by Silien *et al.*,[33] we do not observe any peaks in the dI/dV spectra of Fig. 5 for the C_{60} derived LUMO state at E_F or for other calculated Kohn–Sham states below the Fermi level down to −1.5 eV. We attribute the fact that we do not see a peak in the dI/dV signal directly at the Fermi level to the localization of this C_{60}-derived LUMO state to the lower part of the C_{60} cage and the substrate underneath.

Our DFT calculations reveal that C_{60} strongly bonds to the on-top, hcp-hollow, and fcc-hollow sites of the Cu(111) surface, which apart from the binding energy can be quantified in terms of C—C bond lengths relative to the free C_{60} molecule. For isolated C_{60}, the six-five bond is computed to be 1.459 Å and the six-six bond to be 1.408 Å. These should be compared with the bond lengths listed for all adsorbed configurations in Table I, which are up to 5% longer. The longer C—C bond lengths reflect a strong bonding to the copper surface. Copper-carbon bond lengths are between 2.204 and 2.393 Å.

In the formation of interfacial bonds, electron transfer is from the metal surface to the fullerene. For our model calculation, the total charge transfer is $0.5e$ from copper to the C_{60} molecule based on a Mulliken population analysis; 92% of this charge is localized on the six carbon atoms nearest the copper surface. This does, however, not mean that the rest of the carbons of the cage have no partial charges. Instead, the interfacial charge is somewhat counteracted by positive charges on neighboring carbons of the bottom six-membered ring, and the next layer of carbons above these have slightly negative charges, thus creating a layered charge structure within the fullerene (see Fig. 1), as well as between the fullerene and the metal surface; this effect has also been observed in Ref. 24. The charge transfer from photoemission and near-edge absorption spectrum is estimated to be between $1.5e$ and $2e$.[14,16] Experimentally, the charge transfer is estimated from the interfacial dipole and it is noted that the charge layering complicates the analysis of charge transfer from experiment, in that neglect of the dipoles not directly at the surface can result in an overestimate of total charge transfer. Moreover, the charge transfer may well be different for individually bound molecules compared to monolayers, which show Cu surface reconstruction to different degrees at different deposition and/or annealing temperatures and could mean a difference in the number of Cu—C bonds. On the six-membered ring at the top of a Cu(111) bound C_{60} molecule, the partial charges are zero within the resolution of our calculations, which can be explained by the shielding nature of C_{60} with respect to external fields.[47] In addition, the six-five and six-six bond lengths for this topmost ring are exactly the same as in free C_{60} for all configurations. Together, these facts reveal that the top of the cage is unchanged by the Cu surface bonding,

As can be seen in Table I, our cluster calculations using atom centred Gaussian basis functions and the slab calculations of Wang and Cheng[24] using plane-wave basis functions agree on the C_{60} rotational conformer with the most stable binding on the three Cu(111) binding sites: namely the configurations on-top(III), hcp-hollow(II), and fcc-hollow(II) (see Fig. 3 for nomenclature). However, we will show in Sec. III B that the energy ordering between configurations is not calculated correctly with DFT formulated with either LDA or GGA functionals. For our cluster model surface, buckmin-

sterfullerene above a hollow site is found to be almost as stable as the on-top site. This is especially true at the hcp-hollow site, but we find bonding to the fcc-hollow site to be less favorable. Bonding is only found in C_1 symmetry for the fcc-hollow(II) configuration, and as can be seen from the bond lengths in Table I there is a Jahn–Teller symmetry breaking. Comparing to the corresponding hcp-hollow bonding, we see that the underlying central atom in the second copper layer plays a role in bonding the C_{60}, in that it is pronouncedly displaced toward the surface for the hcp-hollow configurations (i.e., out of the plane of the second layer). The calculations of Wang and Cheng[24] result in similar binding energies for fullerene bonded above the hcp-hollow site, the bridge site, and the fcc-hollow site, but they find a smaller binding energy for the on-top site. We have excluded the bridge site since this site is not C_3 symmetric.

In comparing our STM and DFT data with other calculated and experimental findings, we find discrepancies. For instance, some of the binding configurations reported in Ref. 25 are not plausible, possibly because they used a smaller metal cluster model of the surface and restricted the positions of the metal atoms to be at bulk positions, which has been shown to be a severe approximation since lengthening of the Cu—Cu bonds at the surface has been found for C_{60} bound to Cu(111).[48] However, they do cast doubt on the XPD results in Ref. 12 where the on-top(II) configuration is reported for C_{60} monolayers on Cu(111) as the most stable configuration for individually bound C_{60}. This is also the least stable configuration at this site in our model and in that of Wang and Cheng.[24]

B. C_{60} binding site and rotational configuration from scanning tunneling microscopy manipulations and theory

It is observed from the STM images that the deposited C_{60} molecules have two orientations: This becomes obvious when performing dI/dV maps of several molecules, but it can already be seen in the constant-current image of Fig. 2 as "triangles" with the apex of a triangle pointing "up" and "down." The as-deposited sample has these two orientations in equal proportion. Since it has been shown that triangular features seen in the STM images arise from the molecular orbitals localized on three five-membered rings surrounding the topmost six-membered ring on the C_{60} molecule (Fig. 4), these two configurations relate to C_{60} in two azimuthal orientations differing by a rotation about the C_3 axis of 60°. The STM images, $I(V)$ and dI/dV characteristics, and STS differential conductance images for these two different C_{60} orientations cannot be distinguished from each other except for the orientation itself, which implies that they are identically or nearly identically bound.

The adsorption configurations with C_3 symmetry (labeled as II and II′ in Fig. 3) are pairwise symmetry-equivalent relative to the surface lattice and therefore must have the same energy. Thus, they have to be observed in two azimuthal orientations differing by a rotation about the C_3 axis of 60° with equal probability of occupation. On the other hand, the two observed azimuthal orientations could also be associated with different adsorption sites.

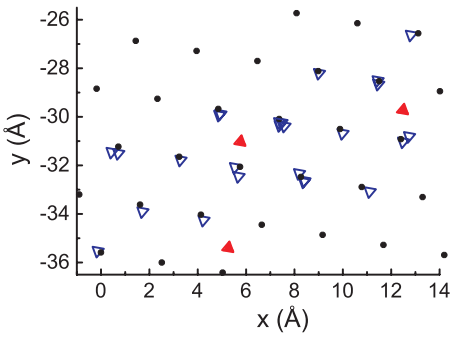

FIG. 6. (Color) A single C_{60} molecule has been manipulated using the STM tip, approaching C_{60} in a succession of manipulations from all sides and angles, and for each movement, the relative position and orientation of the cage has been recorded. The position has been determined with respect to another C_{60} serving as a marker (located at $x=0$ and $y=0$). The blue and red triangles show the resulting positions and orientations. The corners of the triangles point in the directions of the five-membered rings in the upper half of the C_{60} cage. The black dots map out the majority (preferred) hexagonal sublattice as a guide for the eye.

In order to clarify what these two C_{60} orientations signify in terms of Cu(111) binding site and C_{60} rotational configuration, we have performed STM manipulations of individual cages where mapping of the position and molecular azimuthal orientation of a latterly displaced C_{60} molecule relative to other reference C_{60} molecules was performed. This is an extension of the site-mapping technique by using lateral manipulation, as previously applied for a site determination of Cu/Cu(111).[39] In our experiment, an individual C_{60} molecule position is repeatedly displaced by approaching it with the STM tip from different directions and angles; following each manipulation, the displaced new positions are given by the triangles, as shown in Fig. 6. The triangles are colored blue and red depending on the rotational orientations of the molecules. This reveals that the two azimuthal orientations of C_{60} seen in the STM surface scans belong to two *different* hexagonal sublattices on the Cu(111) surface. Both of the hexagonal sublattices that bind C_{60} coincide with the lattice of the topmost layer of the Cu(111). They are shifted with respect to one another by $1/\sqrt{3}$ times the surface lattice constant, as expected for any pair of sublattices out of the three sites: fcc-hollow, hcp-hollow, and on-top sites. This proves that C_{60} binds to two different Cu(111) binding sites in two different rotational orientations.

In a separate experiment, we moved about 50 different C_{60} molecules using STM-manipulation and determined only their azimuthal orientations after the manipulation. Following the STM manipulations, the fractional occupancy of the azimuthal orientations is roughly 1:10, as opposed to a more or less equal distribution of the two azimuthal orientations in the low-temperature as-deposited samples (see Fig. 2). A strong preference for one sublattice after manipulation is found from many different directions for the manipulation, in which different parts of the tip apex are expected to interact with the molecule. We therefore attribute the preference to a slight difference in binding strength between the two orientations on the two sublattices or a slight difference in barrier

height in moving from one binding site to the other.

We can further rule out all of the binding configurations with C_3 symmetry (labeled as II and II′) since they would have to be observed in two azimuthal orientations differing by a rotation about the C_3 axis of 60° with equal probability. By contrast, the manipulation experiment shows one sublattice populated exclusively by upward-pointing triangles. Configurations II and II′ may thus be eliminated.

To see which lattices are populated, we analyze how the azimuthal orientation of the C_{60} molecule relates to the lattice of Cu atoms in the first surface layer. These Cu atoms form rows in the three $\langle 10\bar{1}\rangle$ directions, which point at 60° to one another (see Fig. 3); these directions are also evident in the site mapping in Fig. 6. By recalling that the triangular corners in the STM images are due to the five-membered rings around the top of C_{60}, we examine the effect of rotation of the fullerene in Fig. 3. We find that the azimuthal orientations of the configurations labeled as II and II′ are not in agreement with the orientations found in the experiment. Since these configurations have been already ruled out for symmetry reasons, this is consistent with our site-mapping experiment.

The six C_{3v} configurations, on the other hand, give triangles pointing normal to the $\langle 10\bar{1}\rangle$ Cu rows, for which the configurations with upward- and downward-pointing triangles are symmetry inequivalent with respect to the second layer of Cu: Rotation of 60° transforms configuration I into the nonequivalent configuration III, with different binding energy (Table I). This fits the experimental observation of upward-pointing triangles, favoring one sublattice, and downward-pointing ones, favoring another sublattice on lateral manipulation (Fig. 6) as well as the actual orientations of the intramolecular features with respect to the copper surface lattice. We deduce that one sublattice is populated by configurations labeled as I and the other by configurations labeled as III, and that C_{60} is bonded to Cu(111) in local C_{3v} symmetry.

By referring to the computed energies in Table I, we find the geometries of the fcc-hollow(I) and fcc-hollow(III) configurations to be unstable. This reduces the possible binding configurations to four: on-top(I), on-top(III), hcp-hollow(I), and hcp-hollow(III). Combining these into I/III orientations yields two conformational pairs: (i) on-top(I) and hcp-hollow(III) and (ii) on-top(III) and hcp-hollow(I). Our DFT energies indicate that (ii) is the more likely pair with on-top(III) bonded 809 meV more strongly than hcp-hollow(I). We estimate that the corresponding binding energy difference from Wang and Cheng's[24] study is 140 meV.

Our calculated energetics do not explain why lateral manipulation leads to opposing orientations on two exclusive binding site sublattices. The DFT binding of hcp-hollow(II) is nearly as strong as the global minimum on-top(III), but the experiments exclude hcp-hollow(II) and other II conformers, as discussed above. We attribute this discrepancy to charge localization and electron correlation effects that are not described by the approximate exchange-correlation functionals of DFT with sufficient accuracy. The problem of calculating the relative energy between different binding configurations stems from the multicenter bonding: Many atoms in C_{60} (three or six) bind to several Cu atoms of the substrate surface (three or six) via bonds that are not classical two-center two-electron bonds. It is the intricate balance between C—C, C—Cu, and Cu—Cu bonds of the substrate and adsorbate that differently contribute to different binding configurations and make a definite theoretical prediction difficult. Methods with improved description of electron correlation compared to DFT (e.g., second order Møller–Plesset theory for cluster models or the *GW* approximation for periodic models) in conjunction with a larger basis set would be needed to get also the binding energies in correct order. However, such approaches are too computationally demanding to be tractable for this system size. The fact that DFT gets the C_3 (II) configuration as the most stable on the hcp-hollow site opens up the possibility for the wrong configuration being computed also for the fcc-hollow site, which makes the exclusion of the configurations fcc-hollow(I) and fcc-hollow(III) doubtful. As mentioned above, Wang and Cheng[24] obtained binding energies reconcilable with chemisorption for all rotational conformers of the on-top, hcp-hollow, and fcc-hollow sites (see Table I). This means that four additional I/III combination pairs between on-top and fcc-hollow sites and hcp-hollow and fcc-hollow sites could also explain the STM C_{60} manipulation data of Fig. 6. According to the binding energies of Wang and Cheng[24] (Table I), hcp-hollow(I) and fcc-hollow(III) would be the most probable combination out of these.

C_{60} bonding to metal surfaces for depositions made at elevated temperatures or after annealing is complicated even further, as will be briefly discussed in the following. When monolayers are grown at temperatures around 100 K, two alternating azimuthal orientations of the molecules within the monolayer are observed in experiment. The two alternating orientations correspond to the ones observed for the individual molecules. This is in contradiction with the monolayer structure typically found for annealing at higher temperature.[8,9,11–20] It could well be that the alternating azimuthal orientations correspond to the two alternating binding sites that we have found for the isolated C_{60} molecules on Cu(111). The preferred spacing of the fullerenes in a monolayer could favor an alternating pattern of binding-site occupations that are also associated with different preferred azimuthal orientations. However, when a monolayer is formed, the interaction between neighboring fullerenes may influence the azimuthal orientation of the cages. From our data, we cannot rule out that all molecules of a monolayer adsorb in the same binding site and just alter their azimuthal orientation. Finally, C_{60} bonding to metal surfaces is a complicated matter, as has been seen, e.g., for a C_{60} monolayer on Ag(111),[49] where the binding configuration of the molecules changes depending on the level of K doping.

When we annealed the C_{60} monolayers above room temperature, the molecular orientations of C_{60} in every domain of the film are all the same and these molecules can no longer be easily manipulated with the tip, indicating a stronger bonding. This is in full agreement with the (4×4) structure found in many previous studies after annealing.[8,9,11–20] The annealed films show an increased number of substrate steps underneath the C_{60} film—an indication that the annealing induces a surface reconstruction of the Cu(111) surface.[23]

We therefore believe that the resulting geometry is in this case not related to the monomer experiments.

IV. CONCLUSIONS

We used STM imaging, energy-resolved molecular STS differential conductance spectroscopy, STM molecular manipulation, and DFT modeling to investigate individual C_{60} molecular binding on Cu(111). We have found that C_{60} chemisorbs to the copper surface even when deposited at 5 K. This has been determined through computation of bound C_{60} that displays splitting of its molecular energy levels, which have been mapped to corresponding experimental energy levels via energy-resolved LDOS images. According to the symmetry subgroups of C_{60}, the molecules are bound in either C_{3v} or C_3 symmetry, indicating that they have a six-membered ring facing up and a six-membered ring facing down, both parallel to the surface. Through relating experimental and theoretical energy-resolved STS differential conductance maps of individual C_{60} molecules on the surface, we have identified splitting of the C_{60} derived HOMO and LUMO levels due to chemical bonding and related the triangular features seen in the STM scan images to the triangle formed by the five-membered rings surrounding the six-membered ring at the top of the cage. We have found charge transfer from the surface to the cage in our calculation of partial atomic charges, which is manifested in partial occupation of the C_{60} LUMO. This has been indirectly verified by the close agreement in energy and shape of the experimental and theoretical energy-resolved STS differential conductance images.

STM imaging of many as-deposited molecules shows that C_{60} is bonded to the surface in two different azimuthal orientations in equal proportion, differing in molecular rotation by 60°. We have seen from random STM displacement manipulations of single C_{60} molecules that these two orientations belong to two different hexagonal sublattices, both congruent with the Cu surface lattice. We have through the STM manipulation study shown that one of these sublattices of Cu(111) binding sites is preferred over the other, suggesting that there is a slight difference in binding strength between the two C_{60} azimuthal orientations. We have thus established that C_{60} bonds to Cu(111) in C_{3v} symmetry, with the corners of the triangular features seen in STM scan images pointing normal to the $\langle 10\bar{1}\rangle$ rows of Cu atoms.

Since the relative azimuthal orientation between the two binding configurations is known, we have narrowed the possible pairs of configurations down to two. Of these, DFT predicts that the on-top(III) and hcp-hollow(I) pair is most likely (as defined in Fig. 3). We find that the energy ordering of the C_{60} rotational configurations is not properly described within approximations to DFT, which is attributed to charge localization and electron correlation effects. In light of these shortcomings, other pairs made out of C_{3v} configurations on on-top, hcp-hollow, and fcc-hollow sites are plausible explanations for the experimental observations.

The molecular STM images, $I(V)$ and dI/dV characteristics, and the dI/dV differential conductance images are impossible to tell apart for the two C_{60} binding configurations regardless of azimuthal orientation. This is a testament to the top of the cage being unperturbed by the surface bonding and to the splitting of the C_{60} molecular orbital levels being the same when bound to either binding site.

Both the azimuthal orientation between C_{60} and Cu(111) and the relative azimuthal orientation between different binding sites have been deduced, but we are resigned to the fact that we remain unable to unambiguously determine what binding sites C_{60} bonds at. However, we can limit the possible binding configurations to two pairs. We note that probing the molecular derived unoccupied states of the surface bonded complex provides a sensitive probe to the molecular orientation relative to the surface and for the strength of the charge transfer to the molecule.

ACKNOWLEDGMENTS

We thank Katharina Franke for valuable discussions. J.A.L. wants to thank Nationellt Superdator Centrum (NSC, Sweden) for generous allotment of computer time. J.R. is grateful to the Volkswagen Foundation for funding within the Lichtenberg program. This work was funded in part through the Marie-Curie Human Resources and Mobility Activity (NANOCAGE), the European Union IST project NICE, and Science Foundation Ireland.

*Author to whom correspondence should be addressed; andreas.larsson@tyndall.ie

[1] H. Park, J. Park, A. K. L. Lim, E. H. Anderson, A. P. Alivisatos, and P. L. McEuen, Nature (London) **407**, 57 (2000).
[2] N. Néel, J. Kröger, L. Limot, T. Frederiksen, M. Brandbyge, and R. Berndt, Phys. Rev. Lett. **98**, 065502 (2007).
[3] C. Joachim and J. K. Gimzewski, Chem. Phys. Lett. **265**, 353 (1997).
[4] R. Yamachika, M. Grobis, A. Wachowiak, and M. F. Crommie, Science **304**, 281 (2004).
[5] A. Wachowiak, R. Yamachika, K. H. Khoo, Y. Wang, M. Grobis, D.-H. Lee, Steven G. Louie, and M. F. Crommie, Science **310**, 468 (2005).
[6] X. Lu, M. Grobis, K. H. Khoo, S. G. Louie, and M. F. Crommie, Phys. Rev. Lett. **90**, 096802 (2003).
[7] X. Lu, M. Grobis, K. H. Khoo, S. G. Louie, and M. F. Crommie, Phys. Rev. B **70**, 115418 (2004).
[8] T. Hashizume, K. Motai, X. D. Wang, H. Shinohara, Y. Saito, Y. Maruyama, K. Ohno, Y. Kawazoe, Y. Nishina, H. W. Pickering, Y. Kuk, and T. Sakurai, Phys. Rev. Lett. **71**, 2959 (1993).
[9] T. Hashizume and T. Sakurai, J. Vac. Sci. Technol. B **12**, 1992 (1994).
[10] J. K. Gimzewski, S. Modesti, T. David, and R. R. Schlittler, J. Vac. Sci. Technol. B **12**, 1942 (1994).
[11] T. Sakurai, X. D. Wang, T. Hashizume, V. Yurov, H. Shinohara, and H. W. Pickering, Appl. Surf. Sci. **87/88**, 405 (1995).

[12] R. Fasel, P. Aebi, R. G. Agostino, D. Naumović, J. Osterwalder, A. Santaniello, and L. Schlapbach, Phys. Rev. Lett. **76**, 4733 (1996).
[13] A. Fartash, J. Appl. Phys. **79**, 742 (1996).
[14] K.-D. Tsuei, J.-Y. Yuh, C.-T. Tzeng, R.-Y. Chu, S.-C. Chung, and K.-L. Tsang, Phys. Rev. B **56**, 15412 (1997).
[15] K.-D. Tsuei and P. D. Johnson, Solid State Commun. **101**, 337 (1997).
[16] C.-T. Tzeng, W.-S. Lo, J.-Y. Yuh, R.-Y. Chu, and K.-D. Tsuei, Phys. Rev. B **61**, 2263 (2000).
[17] G. Dutton and X.-Y. Zhu, J. Phys. Chem. B **106**, 5975 (2002).
[18] G. Dutton, J. Pu, D. G. Truhlar, and X.-Y. Zhu, J. Chem. Phys. **118**, 4337 (2003).
[19] G. Dutton and X.-Y. Zhu, J. Phys. Chem. B **108**, 7788 (2004).
[20] K. Motai, T. Hashizume, H. Shinohara, Y. Saito, H. W. Pickering, Y. Nishina, and T. Sakurai, Jpn. J. Appl. Phys., Part 2 **32**, L450 (1993).
[21] T. Sakurai, X. D. Wang, Q. K. Xue, Y. Hasegawa, T. Hashizume, and H. Shinohara, Prog. Surf. Sci. **51**, 263 (1996).
[22] R. Z. Bakhtizin, T. Hashizume, X.-D. Wang, and T. Sakurai, Phys. Usp. **40**, 275 (1997).
[23] W. W. Pai, C.-L. Hsu, M. C. Lin, K. C. Lin, and T. B. Tang, Phys. Rev. B **69**, 125405 (2004).
[24] L. L. Wang and H. P. Cheng, Phys. Rev. B **69**, 045404 (2004).
[25] A. Ogawa, M. Tachibana, M. Kondo, K. Yoshizawa, H. Fujimoto, and R. Hoffmann, J. Phys. Chem. B **107**, 12672 (2003).
[26] M. Abel, A. Dimitriev, R. Fasel, N. Lin, J. V. Barth, and K. Kern, Phys. Rev. B **67**, 245407 (2003).
[27] W. W. Pai and C.-L. Hsu, Phys. Rev. B **68**, 121403(R) (2003).
[28] C.-L. Hsu and W. W. Pai, Phys. Rev. B **68**, 245414 (2003).
[29] M. K.-J. Johansson, A. J. Maxwell, S. M. Gray, P. A. Brühwiler, D. C. Mancini, L. S. O. Johansson, and N. Mårtensson, Phys. Rev. B **54**, 13472 (1996).
[30] R. Felici, M. Pedio, F. Borgatti, S. Iannotta, M. Capozi, G. Ciullo, and A. Stierle, Nat. Mater. **4**, 688 (2005).
[31] A. Stróżecka, J. Mysliveček, and B. Voigtländer, Appl. Phys. A: Mater. Sci. Process. **87**, 475 (2007).
[32] J. I. Pascual, J. Gómez-Herrero, D. Sánchez-Portal, and H.-P. Rust, J. Chem. Phys. **117**, 9531 (2002).
[33] C. Silien, N. A. Pradhan, W. Ho, and P. A. Thiry, Phys. Rev. B **69**, 115434 (2004).
[34] J. I. Pascual, J. Gomez-Herrero, C. Rogero, A. M. Baro, D. Sanchez-Portal, E. Artacho, P. Ordejon, and J. M. Soler, Chem. Phys. Lett. **321**, 78 (2000).
[35] J. J. Perez-Jimenez, J. J. Palacios, E. Louis, E. Sanfabian, and J. A. Verges, ChemPhysChem **4**, 388 (2003).
[36] X. Q. Zhang, W. He, A. D. Zhao, H. N. Li, L. Chen, W. W. Pai, J. G. Hou, M. M. T. Loy, J. L. Yang, and X. D. Xiao, Phys. Rev. B **75**, 235444 (2007).
[37] R. Stadler, S. Kubatkin, and T. Bjornholm, Nanotechnology **18**, 165501 (2007).
[38] M. Casarin, D. Forrer, T. Orzali, M. Petukhov, M. Sambi, E. Tondello, and A. Vittadini, J. Phys. Chem. **111**, 9365 (2007).
[39] J. Repp, F. Moresco, G. Meyer, K.-H. Rieder, P. Hyldgaard, and M. Persson, Phys. Rev. Lett. **85**, 2981 (2000).
[40] A. D. Becke, Phys. Rev. A **38**, 3098 (1988).
[41] J. P. Perdew, Phys. Rev. B **33**, 8822 (1986).
[42] A. Schäfer, H. Horn, and R. Ahlrichs, J. Chem. Phys. **97**, 2571 (1992).
[43] M. Dolg, U. Wedig, H. Stoll, and H. Preuss, J. Chem. Phys. **86**, 866 (1987).
[44] R. Ahlrichs, M. Bär, M. Häser, H. Horn, and C. Kölmel, Chem. Phys. Lett. **162**, 165 (1989).
[45] A. Schäfer, C. Huber, and R. Ahlrichs, J. Chem. Phys. **100**, 5829 (1994).
[46] M. De Menech, U. Saalmann, and M. E. Garcia, Phys. Rev. B **73**, 155407 (2006).
[47] P. Delaney and J. C. Greer, Appl. Phys. Lett. **84**, 431 (2004).
[48] C. Ton-That, M. E. Welland, J. A. Larsson, J. C. Greer, A. G. Shard, V. R. Dhanak, A. Taninaka, and H. Shinohara, Phys. Rev. B **71**, 045419 (2005).
[49] A. Tamai, A. P. Seitsonen, R. Fasel, Z.-X. Shen, J. Osterwalder, and T. Greber, Phys. Rev. B **72**, 085421 (2005).